NASA TND-1338

NASA TND-1338

TECHNICAL NOTE

D-1338

PRELIMINARY RESULTS OF RADIATION MEASUREMENTS FROM THE TIROS III METEOROLOGICAL SATELLITE

W. Nordberg, W. R. Bandeen,
B. J. Conrath, V. Kunde and I. Persano

Goddard Space Flight Center
Greenbelt, Maryland

NATIONAL AERONAUTICS AND SPACE ADMINISTRATION
WASHINGTON
May 1962

PRELIMINARY RESULTS OF RADIATION MEASUREMENTS FROM THE TIROS III METEOROLOGICAL SATELLITE

by
W. Nordberg, W. R. Bandeen,
B. J. Conrath, V. Kunde and I. Persano
Goddard Space Flight Center

SUMMARY

Three simple and typical cases of radiation fluxes measured by the TIROS III meteorological satellite are presented and discussed. These cases deal with emitted earth radiation received in three infrared bands and reflected solar radiation received in two visible bands over the tropical Atlantic, the eastern United States, and the North African desert. Each case is accompanied by results from a wide-field radiometer and photographs from TV cameras flown in the same satellite. The cases over the Atlantic Ocean and the African desert were in almost cloudless skies, while the case over the United States included regions ranging from heavily clouded to clear. Results show that the measurements from the various instruments and in the various channels are internally consistent. Maximum albedo values over the overcast areas were determined to be approximately 55 percent. Over the ocean, albedos were near 7 percent, and over land and clear skies the albedo varied from about 15 percent over heavy vegetation to about 30 percent over the desert. Total outgoing energy fluxes in the infrared were computed to be as high as 340 w/m^2 over the desert and as low as 190 w/m^2 over the cloudy areas. With the exception of the measurements made over the desert, results in the atmospheric window channel (7.5 to 13.5 μ) show substantial absorption, probably due to water vapor.

CONTENTS

Summary i

INTRODUCTION. 1

DESCRIPTION OF THE SENSORS 2

PHYSICAL DEFINITION OF THE MEASUREMENTS 3

THE RADIATION PATTERNS 5

The Tropical Atlantic Ocean (Clear Skies) 5
The Eastern United States (Cloudy Skies) 11
The North African Desert (Clear Skies) 15

CONCLUSION 21

References 22

PRELIMINARY RESULTS OF RADIATION MEASUREMENTS FROM THE TIROS III METEOROLOGICAL SATELLITE*

by
W. Nordberg, W. R. Bandeen,
B. J. Conrath, V. Kunde and I. Persano
Goddard Space Flight Center

INTRODUCTION

TIROS III is the third in a series of meteorological satellites successfully placed into near-circular orbits (approximate altitude 780 km) by NASA. It is the second satellite to carry sensors for the measurement of infrared radiation emitted and solar radiation reflected from the earth.

This report discusses: simultaneous measurements of the earth's apparent blackbody temperature and its albedo from the wide-field radiometer, and of the radiant emittances and albedos in the spectral regions covered by the five-channel radiometer. These measurements were made over the tropical Atlantic Ocean and North Africa, both under clear skies, and over the eastern United States under cloudy skies. In all three cases the data were taken near local noon. The radiation measurements are accompanied by simultaneous TV photographs made by TIROS III over the same areas.

No attempt will be made here to present any conclusions in regard to the overall and quantitative heat balance of the planet or to radiative transmission characteristics of the atmosphere which might be derived from these measurements. Although a sufficient quantity of data has been transmitted from both TIROS II and TIROS III to make such conclusions feasible, it is necessary first to study a few sample cases and interpret them within the framework of existing knowledge. At the same time, a comparison of the simultaneous measurements from all sensors for these few simple cases permits a test of the internal consistency of the whole experiment.

The cases presented here have been chosen purely to establish examples for further studies, and to demonstrate the potential which these data provide for large-scale analyses

*Published in *Journal of Atmospheric Sciences* (formerly *Journal of Meteorology*), 19, (1); 20–29 January 1962

of the planetary heat budget or for the investigation of radiation patterns connected with the development and dynamic behavior of meteorological circulation systems. Such analyses may even be applied to similar measurements made on other planets and thus make these measurements more meaningful. These analyses can only be carried out with the aid of electronic computing machines, since they must make use of a fantastically large amount of data, an amount which is steadily increasing. For example, approximately 200,000 radiation data words are being transmitted per orbit and several hundred millions of data words have already accumulated from TIROS II and III together.

Similar results have been published previously for the TIROS II satellite (References 1, 2, and 3). However, a presentation of the TV photographs together with all types of radiation data is attempted for the first time with the TIROS III measurements because of the excellent quality of the TV pictures and of experience gained in improving the calibration, especially of the visible radiation channels and of the wide-field radiometer.

DESCRIPTION OF THE SENSORS

The sensors carried in the satellite are identical to the ones flown in TIROS II, and have been described previously by Bandeen, et al. (Reference 4). They form two instruments. The first is a non-scanning radiometer with a broad response in both the visible and infrared regions and a rather low spatial resolution. Its aperture is approximately 55 degrees. The second is a scanning radiometer which scans as the satellite spins. It is of medium spatial resolution, has a 5 degree aperture, and responds to radiation in five different spectral regions which are separated by optical filters. Three of these regions are in the infrared between 5.9 and 6.7 microns, between 7.5 and 13.5 microns, and between 7.0 and 32.0 microns. The other two regions lie mainly in the visible portion of the spectrum, that is, between 0.50 and 0.75 microns and between 0.2 and 7.0 microns. These spectral regions are purely nominal since the response of the instrument within these regions is far from flat; therefore, the exact spectral response curves must be used when the energy distribution in each channel is calculated. These curves have been published previously (Reference 5).

In the 5.9 to 6.7 micron channel a maximum of absorption due to water vapor is encountered. Energy in this channel is therefore received mainly from the highest altitudes where water vapor may be found in the atmosphere. In contrast, the optical depth is a maximum in the 7.5 to 13.5 micron channel, since absorption due to any of the atmospheric constituents—except ozone which covers only a minor portion of this channel—is very small. The 7.0 to 32.0 micron channel covers almost 80 percent of the total blackbody energy emitted by the earth, while the total solar energy reflected from the earth is contained in the 0.20 to 7.0 micron channel. The 0.50 to 0.75 micron channel is of interest because it covers only a narrow spectral region very near the maximum

of the solar energy distribution, and it is similar in its spectral response to the TV cameras carried on the same satellite.

One of the basic differences between the wide-field and the five-channel instruments is that the five-channel radiometer scans the earth during all portions of the orbit, while the wide-field radiometer fully views the earth during less than a fifth of the orbit. The wide-field instrument measures the radiant emittance of a target by means of a thermistor whose resistance is a function of the absorbed energy flux. This is accomplished over the whole spectrum with two detectors: a black one equally sensitive to radiation emitted and reflected from the earth, and a white one predominantly sensitive to emitted radiation. The portion of solar energy reflected from the earth (the earth's albedo) and the apparent blackbody temperature for the earth can be determined by comparing the energies received by the black and white detectors. A complete description of this instrument has been given by Hanel (Reference 6).

Very much in contrast to the wide-field radiometer, the sensors in the five-channel instrument are alternately, and in rapid succession, illuminated with two diametrically opposed fields of view, one scanning the earth and the other pointing into outer space. The sensors therefore measure the difference of the energy fluxes in the two directions. Since the flux from outer space is essentially zero, this serves as a reliable reference.

A detailed description of this instrument and its scanning mechanism is contained in Reference 4. Further instrumental details, such as recording, transmitting and electrical conversion of the measurements have been described in Reference 7.

PHYSICAL DEFINITION OF THE MEASUREMENTS

The results are derived by interpreting the output of the radiometers in terms of energy fluxes emitted and reflected by the earth in the direction viewed by the sensors. A complex calibration procedure (References 4 and 5) determines the relation between output and energy flux. For the visible (reflected solar radiation) channels of the five-channel radiometer, this relation is established by illuminating the sensors with a diffusely radiating source of known spectral distribution and total radiance. Since the spectral response of the radiometer is assumed to be known from the spectral characteristics of the individual reflecting, refracting and transmitting components of the optic, that portion of the radiant emittance of the source which falls within the spectral response curve of the instrument can be calculated (Reference 5). This value is termed $\overline{W}$.

It is in terms of this quantity, expressed in watts per square meter, that the sensor is calibrated. Then a computation is made of the radiant emittance which would result within the same spectral curve if a diffuse reflector of a certain albedo were illuminated by the sun at a given angle of incidence. This computation is compared with every

measurement obtained by the satellite, where a blackbody temperature of 5800°K and a total flux of 1,400 watts per square meter are assumed for the sun. The energy flux measured by the satellite sensor, expressed as a percentage of this solar flux, is called the measured albedo.

The wide-field radiometer is also calibrated with a diffuse source of known intensity. But in this case, the spectral response of the instrument is assumed to be uniform over the visible region and the intensity of the source is therefore expressed directly as a percentage of diffusely reflected solar energy. Except for the angle of solar incidence, for which a correction must be made for every satellite position, the output of the wide-field radiometer may be expressed directly in terms of albedo.

A different procedure is employed for the calibration of the thermal (emitted radiation) channels. Here the radiometer is exposed to a blackbody source of known temperature. In the case of the wide-field radiometer, whose spectral response in the infrared is not precisely known, the output is simply expressed in terms of these blackbody temperatures; this instrument therefore measures the apparent blackbody temperatures of the viewed areas. For the five-channel radiometer, the spectral response curve of each sensor is again assumed to be known from the response of each individual component of the optic. Again, as in the case of the visible channels, that portion of the radiant emittance of the blackbody which falls within the spectral response curve of each channel is determined. This is accomplished by integrating the Planck function over the spectral response curve. The results $\overline{W}$ of this integration for all three channels are presented in Figure 1.

The data from these three thermal channels can therefore be expressed either in degrees Kelvin or in watts per square meter of radiant emittance within the spectral curve of a specific channel. In the cases presented here, all thermal results are given as blackbody temperatures. This facilitates comparison of the data between the two radiometers and permits interpretation of the data from the 7.5 to 13.5 micron channel which, in the absence of clouds, should yield blackbody temperatures very close to surface temperatures of the earth. All blackbody temperatures for these three thermal channels can be converted into energy fluxes by means of the curves shown in Figure 1.

It should be pointed out that the energy fluxes thus obtained in the three thermal channels do not appear to be very meaningful because the measured radiant emittances are concealed by very complicated nonuniform spectral responses (Reference 5).

Fortunately, however, Wark and Yamamoto (Reference 8) have shown that—at least in the 7 to 32 micron channel—an approximately linear relation exists between the energy flux per steradian measured by the nonuniformly responding TIROS sensor and the total flux per steradian radiated by the earth in the direction of the satellite. The relation between the latter value and the total flux radiated by the earth over a hemisphere has

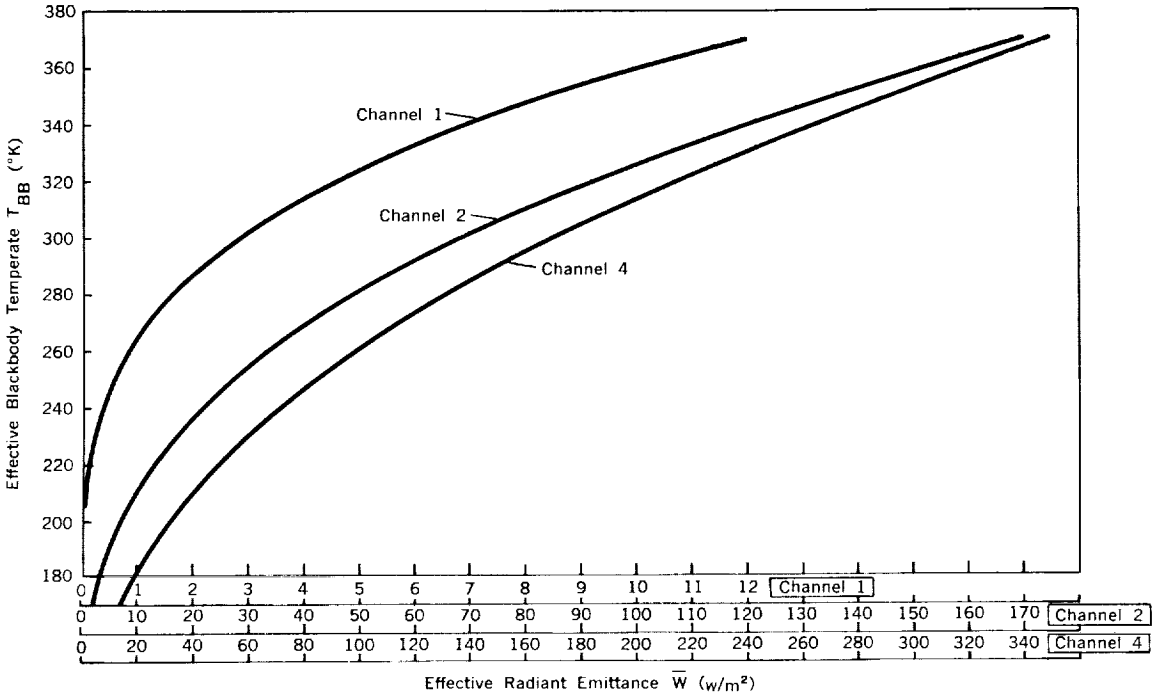

Figure 1—Effective blackbody temperature versus effective radiant emittance for channels 1, 2, and 4 of the TIROS III medium resolution radiometer

not been completely established as yet, but a fairly good approximation can probably be made merely by multiplying by π where the satellite measurements were made under nadir-angle conditions of 45 degrees or less.

In all cases presented here, the satellite was oriented so that both the wide-field radiometer and the TV cameras viewed the earth's surface very nearly vertically while the nadir angles for the five-channel radiometer scans varied between 0 and 45 degrees except for scans very near the horizon. Thus, it can be assumed that these measurements are representative of the outward fluxes of energy over the areas viewed within the spectral regions specified. For the sake of clarity in illustrating the three cases, only half of the data points actually analyzed are shown in the plots.

THE RADIATION PATTERNS

The Tropical Atlantic Ocean (Clear Skies)

A very simple case is presented in Figures 2 through 8. The photograph (Figure 2) of the area viewed by the satellite shows the Atlantic Ocean off the coast of South America. The shoreline can be seen in the upper left-hand corner of the photograph.

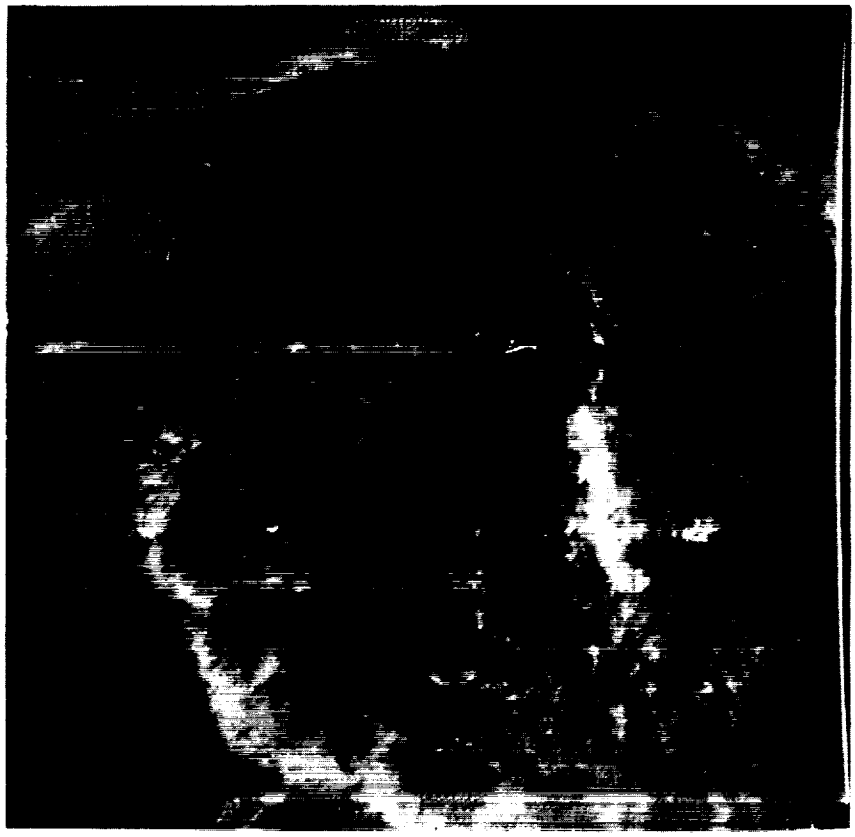

Figure 2—Photograph taken by TIROS III during Orbit 117 at about 1444 GMT on July 20, 1961. The coast of South America is visible.

With the exception of some minor scattered clouds, the sky is clear. Nevertheless, the blackbody temperatures measured by the 7.5 to 13.5 micron channel shown in Figure 4 are some 20° K lower than the expected water temperature in this area. This suggests that even within this so-called "atmospheric window" region of the spectrum there is a considerable absorption of energy, probably due to water vapor since there is not sufficient ozone to decrease the blackbody temperatures by 20°K. There must be a very large amount of water vapor in this area to decrease the radiant emittance in this spectral region by approximately 25 percent. The low outward energy flux is also indicated by Figures 3 and 6 which show the equivalent blackbody temperatures for the 5.9 to 6.7 micron channel and the 7.0 to 32.0 micron channel, respectively. Furthermore, as might be expected over the ocean, the reflected solar energy measured in the 0.2 to 7 and the 0.50 to 0.75 micron channels (Figures 5 and 7, respectively) is very low. The sink of energy in this area is of particular interest since Hurricane Anna, which is off the top of the photograph (Figure 2), had developed previously in the same general area.

The discrepancy in the albedo values obtained in the 0.5 to 0.75 micron region (7 percent) and the 0.2 to 7 micron region (4 percent) is noteworthy, especially since,

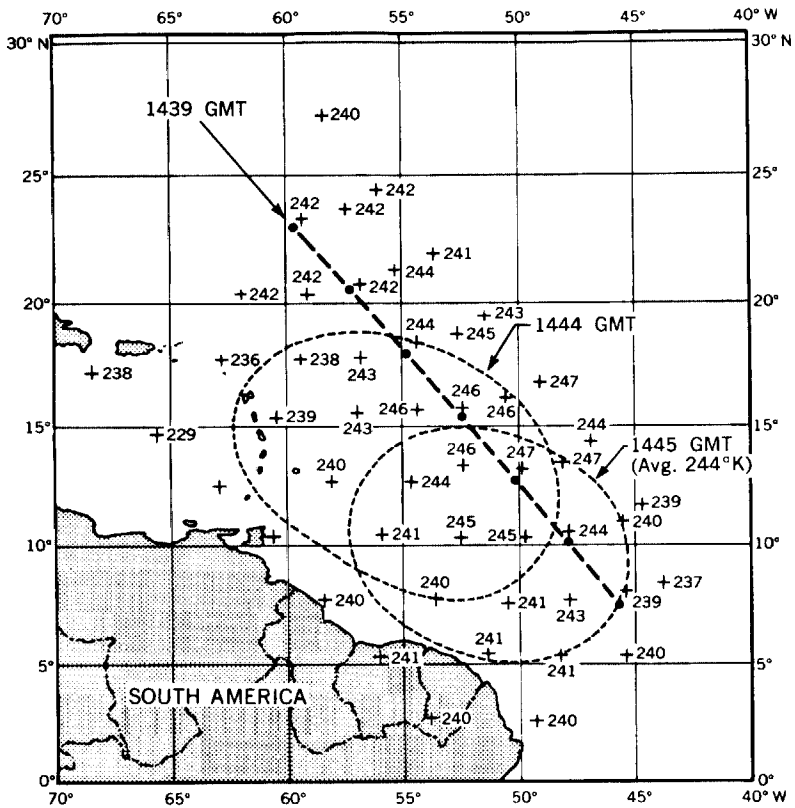

Figure 3—Effective blackbody temperatures (°K) measured by channel 1 (approximately 5.9 - 6.7μ) of the medium resolution radiometer between 1439 and 1445 GMT, Orbit 117, July 20, 1961. Averages of these data are given for the areas enclosed by dashed lines (also viewed by the low-resolution wide-field radiometer at the times shown). The heavy dashed line is the subsatellite path with points each minute.

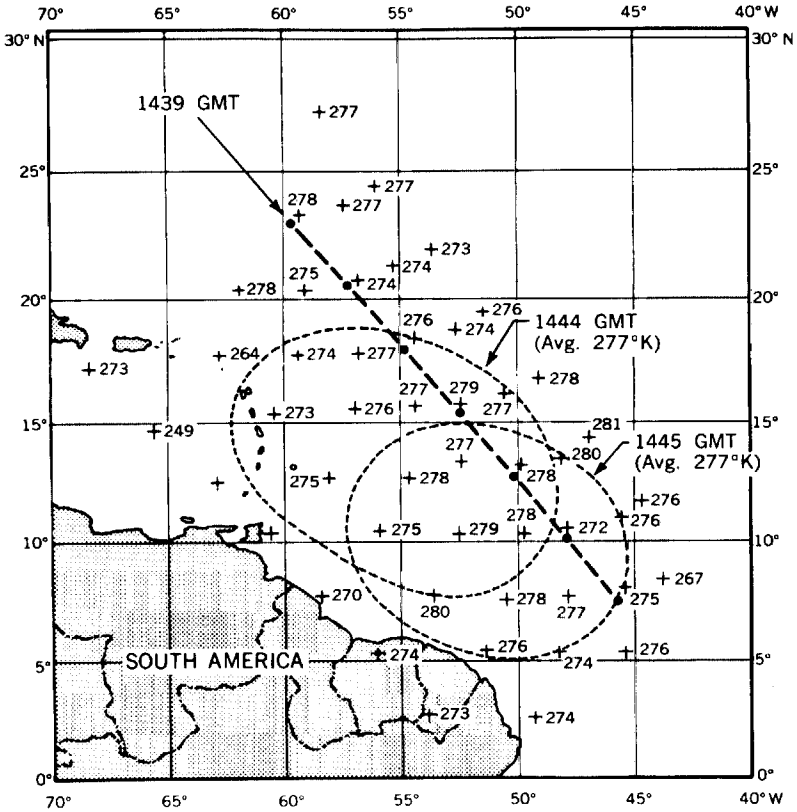

Figure 4—Effective blackbody temperatures (°K) measured by channel 2 (approximately 7.5 - 13.5μ) of the medium resolution radiometer between 1439 and 1445 GMT, Orbit 117, July 20, 1961. Averages of these data are given for the areas enclosed by dashed lines (also viewed by the low-resolution wide-field radiometer at the times shown). The heavy dashed line is the subsatellite path with points each minute.

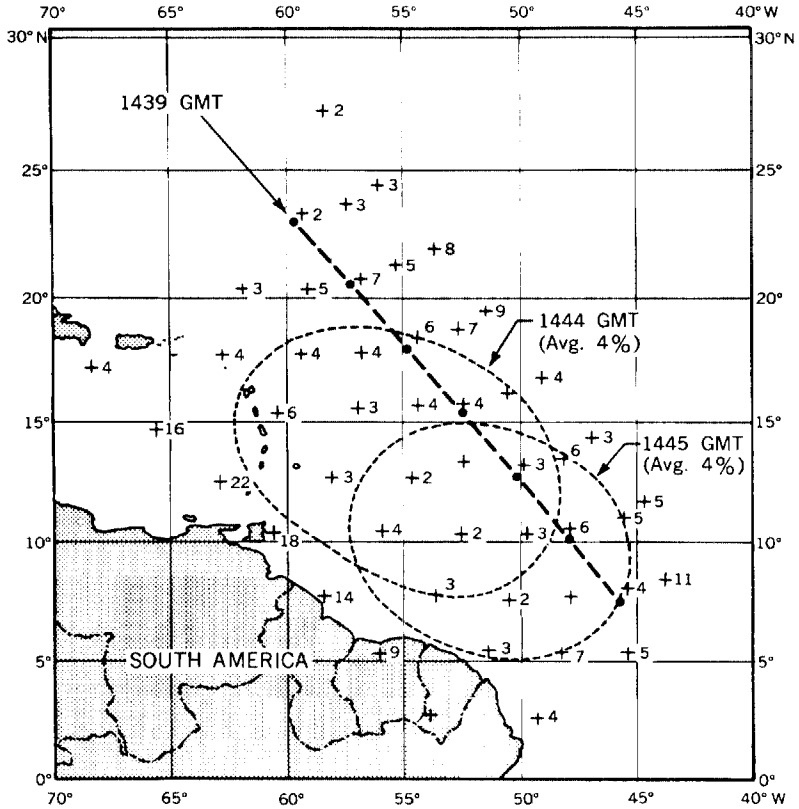

Figure 5—Albedo percentages measured by channel 3 (0.2 - 7.0 μ) of the medium resolution radiometer between 1439 and 1445 GMT, Orbit 117, July 20, 1961. Averages of these data are given for the areas enclosed by dashed lines (also viewed by the low-resolution wide-field radiometer at the times shown). The heavy dashed line is the subsatellite path with points each minute.

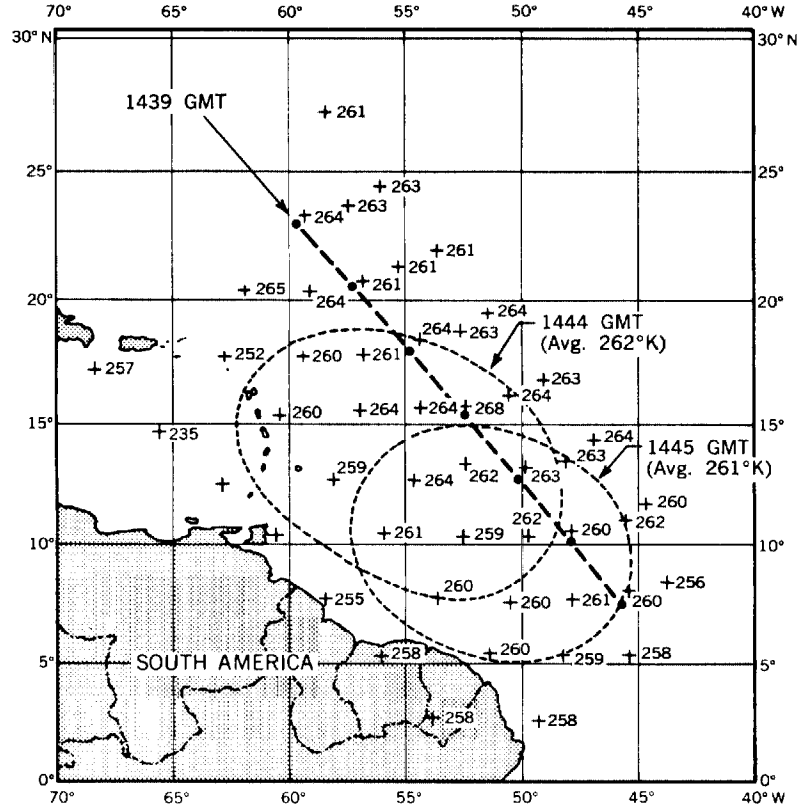

Figure 6—Effective blackbody temperature (°K) measured by channel 4 (approximately 7.0 - 32.0 μ) of the medium resolution radiometer between 1439 and 1445 GMT, Orbit 117, July 20, 1961. Averages of these data are given for the areas enclosed by dashed lines (also viewed by the low-resolution wide-field radiometer at the times shown). The heavy dashed line is the subsatellite path with points each minute.

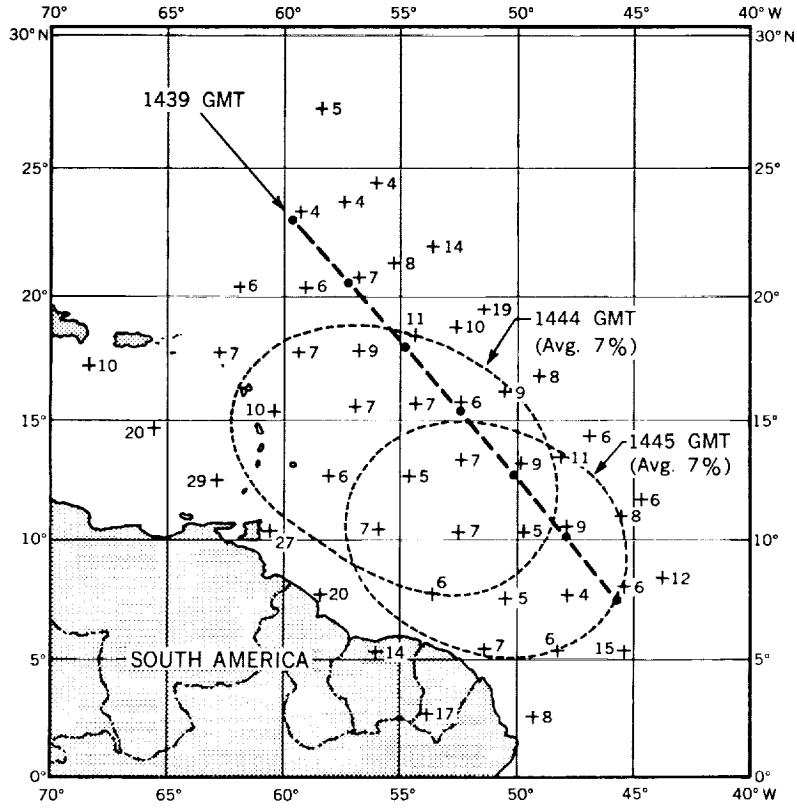

Figure 7—Albedo percentages measured by channel 5 (approximately 0.5 — 0.75μ) of the medium resolution radiometer between 1439 and 1445 GMT, Orbit 117, July 20, 1961. Averages of these data are given for the areas enclosed by dashed lines (also viewed by the low-resolution wide-field radiometer at the times shown). The heavy dashed line is the subsatellite path with points each minute.

as may be seen below, it exists in all other cases. There could be several reasons for this. One reason is that more nearly diffuse reflection prevails in the narrow region from 0.5 to 0.75 microns, while in the broader region from 0.2 to 7 microns, losses of energy are encountered due to other processes. These processes might conceivably be selective absorption in the infrared end of the visible region, or atmospheric scattering in the ultraviolet end, or both. The fact, however, that such a discrepancy has been observed in all three of the cases studied here does not conclusively prove this reasoning. A more complete investigation of all TIROS III data will be made to explore this problem further. There is a greater probability that this discrepancy may be introduced by the instrument itself. The visible channels are calibrated with a standard source whose spectral distribution peaks between 1 and 2 microns. Because of the great

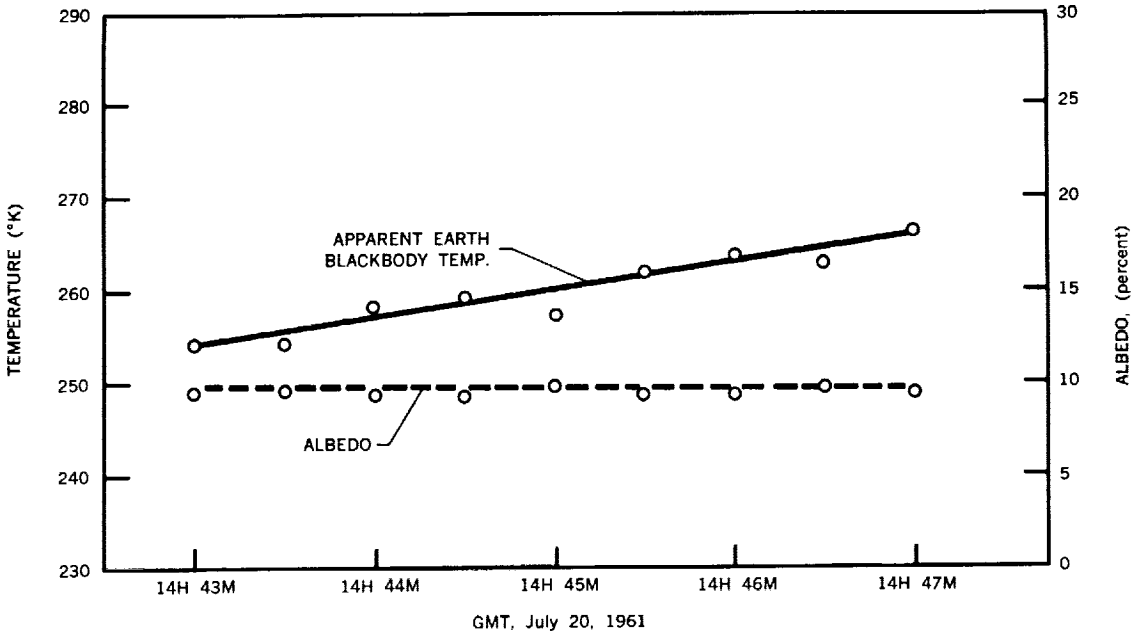

Figure 8—Apparent earth blackbody temperature and albedo versus time measured by the TIROS III wide-field radiometer during Orbit 117

difference in spectral response between the two channels (Reference 5), an error in the knowledge of the spectral distribution of the source within a certain range may have more effect on one channel than on the other. This error is most likely to appear in the 0.2 to 7 micron channel.

The wide-field radiometer yields a constant albedo value of about 9 percent between 1443 and 1447 GMT (Figure 8). This corresponds well with the average value of 7 percent measured by the 0.5 to 0.75 micron channel over the same areas (dashed circles in Figure 7). It also indicates a possible calibration error in the 0.2 to 7 micron channel whose values in this area average only 4 percent, yet the spectral response of the 0.2 to 7 micron channel rather than the response of the 0.5 to 0.75 micron channel is similar to that of the wide-field radiometer. This better agreement between the wide-field data and the "narrow" channel rather than the "broad" one, which similarly holds for the two cases discussed below, does not support the foregoing assumption of spectral variation in atmospheric reflectance, but rather that of a calibration error in the "broad" channel.

It should be noted that the albedo values from both channels trace out the approximate shoreline of the South American continent and the cloudy area near the top of the photograph (Figure 2). The albedos for the land portions are about 9 percent and 16 percent from the 0.2 to 7 micron channel and the 0.5 to 0.75 micron channel, respectively. For the cloudy portion, they are about 22 and 30 percent, respectively.

The apparent blackbody temperature of about 258° and 260°K obtained from the wide-field radiometer at 1444 and 1445 GMT, respectively (Figure 8) agree fairly well with the averages of 262° and 261° K given by the 7.0 to 32.0 micron channel for the same times. The wide-field radiometer covers approximately the same spectral range as this channel. The rising trend in the wide-field temperatures (Figure 8) is probably due to the time constant of this instrument which had just previously viewed portions of outer space as well as the very cold cloudy areas to the north.

The Eastern United States (Cloudy Skies)

Another case is presented in Figure 9 through 15. The photograph (Figure 9) shows the Michigan peninsula and Great Lakes in the lower right-hand corner and a large cloud mass in the center. The maximum albedo values measured over the densest portion of the overcast area are 35 to 40 percent and 50 to 55 percent in the "broad" and "narrow" visible channels respectively. The approximate values for the cloudless band

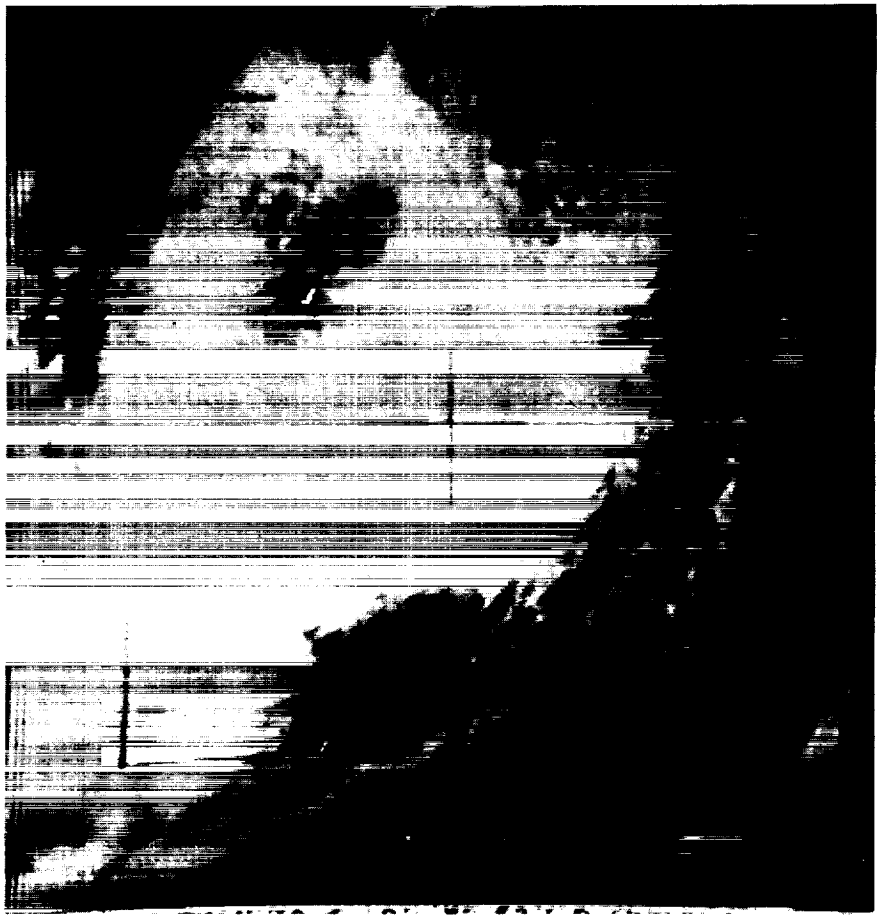

Figure 9—Photograph taken by TIROS III during Orbit 4 at about 1735 GMT on July 12, 1961, while over Kentucky. Michigan and the Great Lakes are visible.

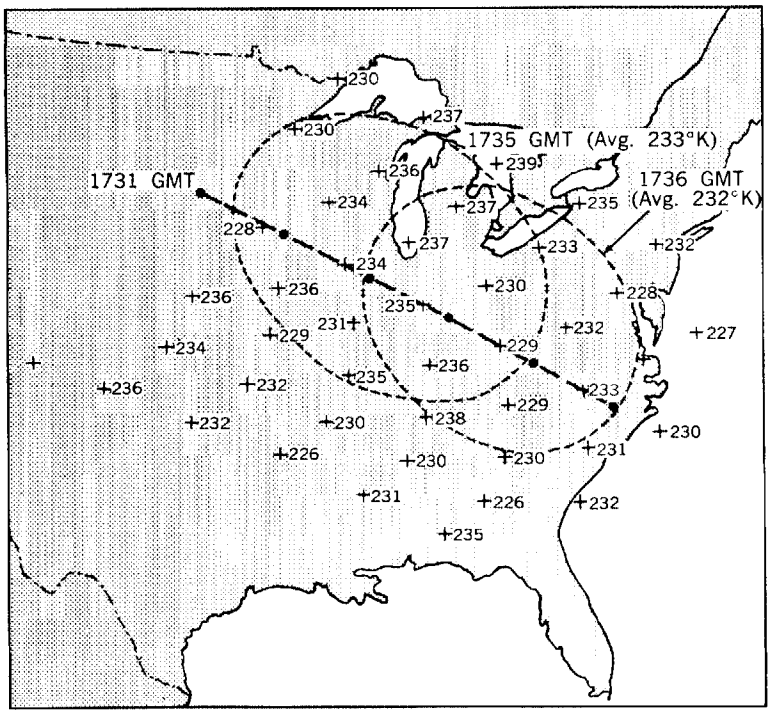

Figure 10—Effective blackbody temperature (°K) measured by channel 1 (approximately 5.9 - 6.7μ) of the medium resolution radiometer between 1731 and 1736 GMT, Orbit 4, July 12, 1961. Averages of these data are given for the areas enclosed by dashed lines (also viewed by the low-resolution wide-field radiometer at the times shown). The heavy dashed line is the subsatellite path with points each minute.

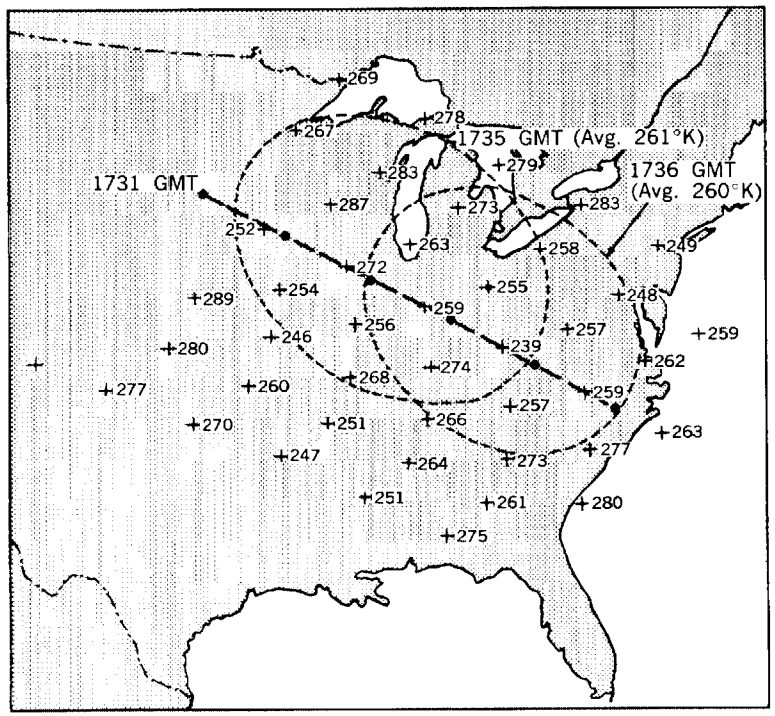

Figure 11—Effective blackbody temperature (°K) measured by channel 2 (approximately 7.5 - 13.5μ) of the medium resolution radiometer between 1731 and 1736 GMT, Orbit 4, July 12, 1961. Averages of these data are given for the areas enclosed by dashed lines (also viewed by the low-resolution wide-field radiometer at the times shown). The heavy dashed line is the subsatellite path with points each minute.

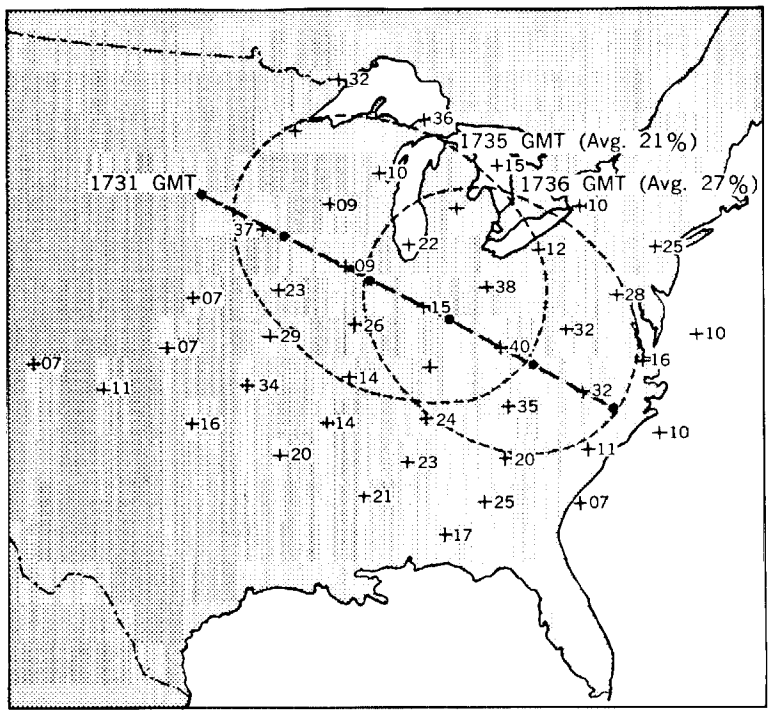

Figure 12—Albedo percentages measured by channel 3 (approximately 0.2 - 7.0μ) of the medium resolution radiometer between 1731 and 1736 GMT, Orbit 4, July 12, 1961. Averages of these data are given for the areas enclosed by dashed lines (also viewed by the low-resolution wide-field radiometer at the times shown). The heavy dashed line is the subsatellite path with points each minute.

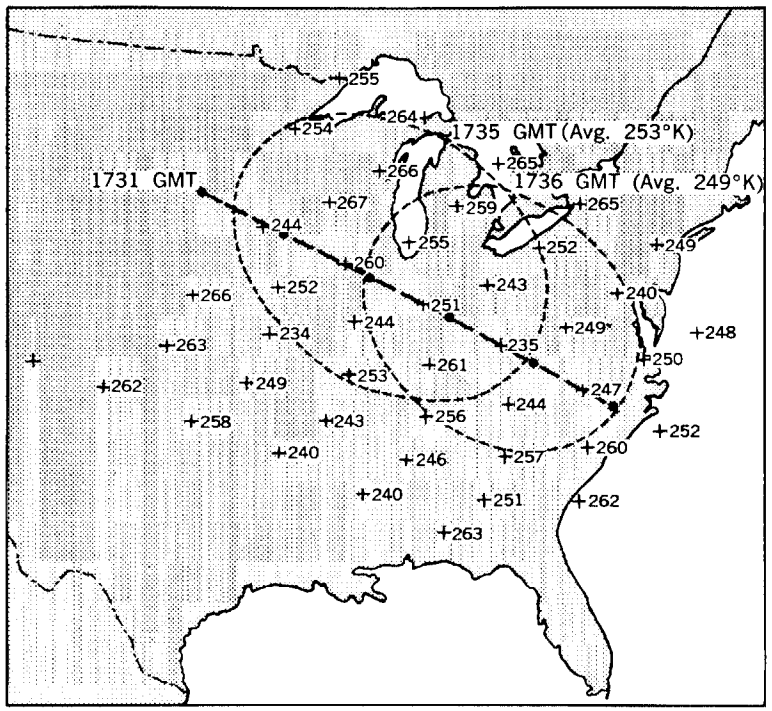

Figure 13—Effective blackbody temperatures (°K) measured by channel 4 (approximately 7.0 - 32.0μ) of the medium resolution radiometer between 1731 and 1736 GMT, Orbit 4, July 12, 1961. Averages of these data are given for the areas enclosed by dashed lines (also viewed by the low-resolution wide-field radiometer at the time shown). The heavy dashed line is the subsatellite path with points each minute.

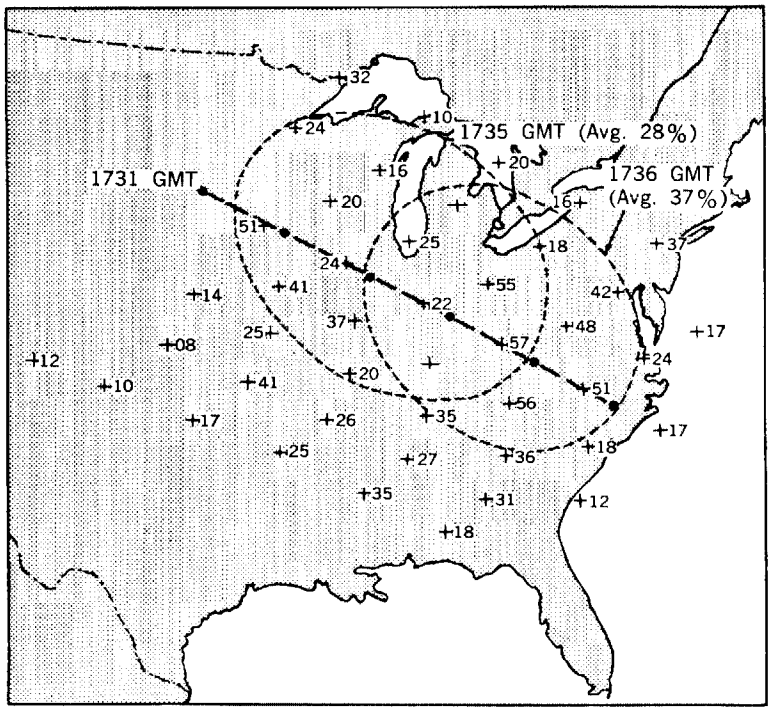

Figure 14—Albedo percentages measured by channel 5 (approximately 0.50 - 0.75 μ) of the medium resolution radiometer between 1731 and 1736 GMT, Orbit 4, July 12, 1961. Averages of these data are given for the areas enclosed by dashed lines (also viewed by the low-resolution wide-field radiometer at the times shown). The heavy dashed line is the subsatellite path with points each minute.

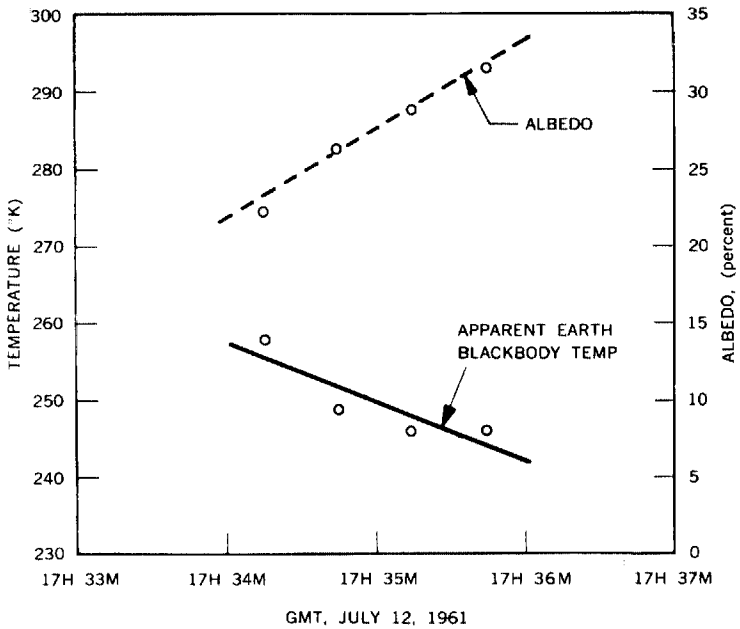

Figure 15—Apparent earth blackbody temperature and albedo versus time measured by the TIROS III wide-field radiometer during orbit 4

of land just to the northwest of the overcast area (Michigan, Wisconsin, Illinois) are correspondingly 8 to 12 percent and 15 to 20 percent (Figures 12 and 14). This is very similar to the values obtained over the coastline of South America in the case above. The average values over the areas indicated by the circle in Figures 12 and 14 are 21 and 28 percent for the "broad" and "narrow" channels, respectively, in one area (circles marked 1735); and 27 and 37 percent, respectively, in the other area (circles marked 1736). The wide-field radiometer values for these corresponding areas are 26 and 32 percent.

The thermal channels indicate extremely low infrared energy fluxes over the whole area. Over the dense clouds the "window" channel measures minimum temperatures as low as 239°K (Figure 11). This indicates very high cloud altitudes, while the 5.9 to 6.7 micron channel (Figure 10) shows minimum temperatures still 10 degrees lower. The 7.0 to 32.0 micron channel shows minimum blackbody temperatures of about 235°K (Figure 13). Over the clear skies the corresponding maximum blackbody temperatures are 283°K, 236°K, and 266°K for the 7.5 to 13.5, the 5.9 to 6.7, and the 7.0 to 32.0 micron channels, respectively. Even over these clear areas, the water vapor in the atmosphere apparently still keeps the outward flux of energy at a fairly low level, a level which is comparable to the one observed in the previous case over the tropical Atlantic Ocean. The blackbody temperatures obtained from the wide-field radiometer are 250°K at 1735 GMT and 243°K at 1736 GMT (Figure 15). Again, this is comparable to the temperatures of 253°K and 249°K for the 7.0 to 32.0 micron channel averaged over the areas shown in Figure 13.

The North African Desert (Clear Skies)

The most interesting of the three cases discussed here is presented in Figures 16 through 24. The three photographs (Figure 16, 17 and 18) show the satellite passing from the cloudless Mediterranean Sea (Figure 16) over the Libyan desert (Figure 17) into the highlands near the Sudan-Ethiopian border (Figure 18). The dark area in the lower right corner of Figure 16 shows the Libyan Uplands near El Haruj. This area is detected by the albedo channels of the five-channel radiometer. Albedo values in this area drop to about 16 percent for the "broad" channel and to about 18 percent for the "narrow" channel, while albedos for the surrounding desert region are 21 and 27 percent respectively (Figure 21 and 23). The wide-field radiometer (Figure 24) shows a steady increase of albedo from 14 percent to about 29 percent between 1053 GMT and 1058 GMT as the field of view moves from the Mediterranean Sea into the brightly reflecting desert regions (Figure 17). It shows a decrease again to about 15 percent after the field of view has left the African continent and views the eastern portion of the Indian Ocean (1105 GMT).

Figure 16—Photograph taken by TIROS III during Orbit 43 at about 1052 GMT, July 15, 1961. The coast of Libya and the Mediterranean Sea are clearly visible.

The steadily increasing wide-field radiometer albedo values of 14, 16, 20, and 26 percent at 1054, 1055, 1056, and 1057 GMT, respectively, again are comparable to the average values of about 27 percent obtained from the "narrow" channel of the five-channel radiometer (Figure 23), considering the relatively long time constant of the wide-field instrument (approximately 1.5 minutes). Over the more heavily vegetated areas of the Blue Nile, the albedo drops to an average of about 15 percent for the "broad" channel and about 20 percent for the "narrow" channel, while over the apparently cloudy regions of the central Sudan it increases to about 30 and 40 percent, respectively (Figures 21 and 23). This contrast in albedos is also expressed in the TV photographs (Figures 17 and 18) and in the wide-field data which, again considering the time delay, undergo a minimum over the Blue Nile valley (1059.5 GMT in Figure 24), and a maximum again over Ethiopia (1102 GMT).

The thermal channels in this case show a most interesting behavior. Over the desert region, the "window" channel is mostly saturated near 310°K (Figure 20). This temperature is probably very close to the surface temperature, indicating the absence of

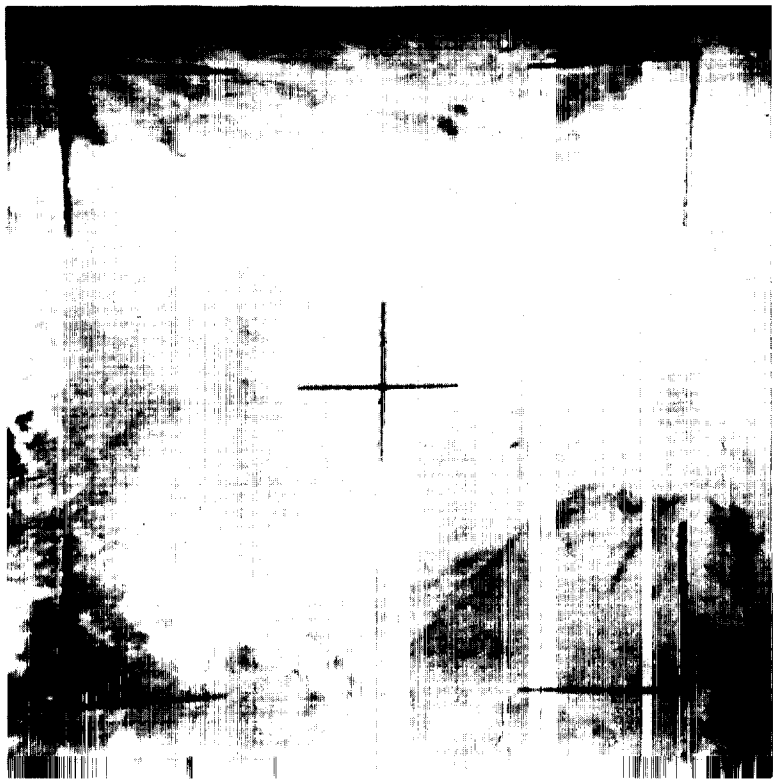

Figure 17—Photograph taken by TIROS III during Orbit 43 at about 1057 GMT, July 15, 1961, showing arid desert regions in the northwestern Sudan

Figure 18—Photograph taken by TIROS III during Orbit 43 at about 1059 GMT, July 15, 1961, over the forested and partly cloudy region in the vicinity of the Nile River in the Eastern Sudan

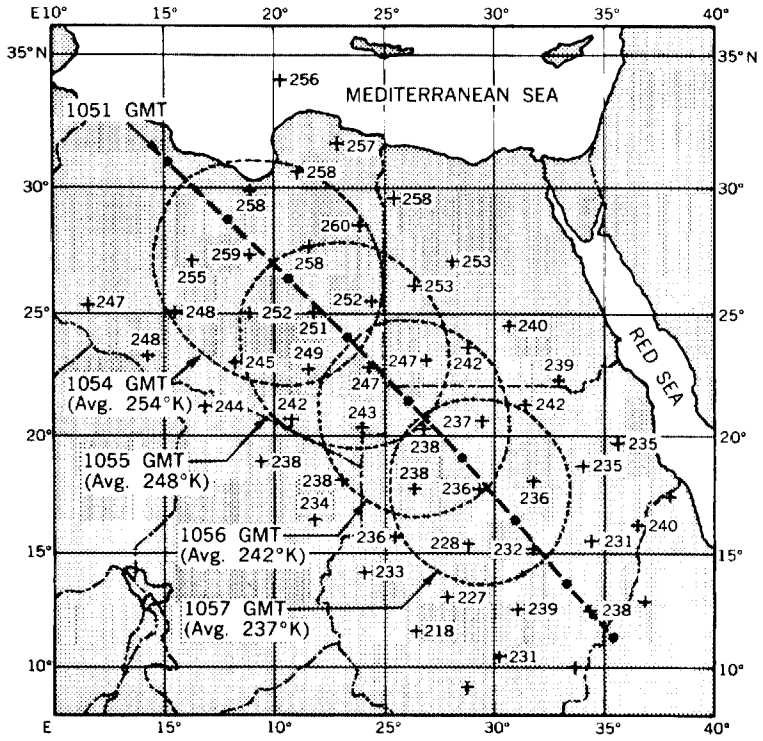

Figure 19—Effective blackbody temperatures (°K) measured by channel 1 (approximately 5.9 - 6.7μ) of the medium resolution radiometer between 1051 and 1057 GMT, Orbit 43, July 15, 1961. Averages of these data are given for the areas enclosed by dashed lines (also viewed by the low-resolution wide-field radiometer at the times shown). The heavy dashed line is the subsatellite path with points each minute.

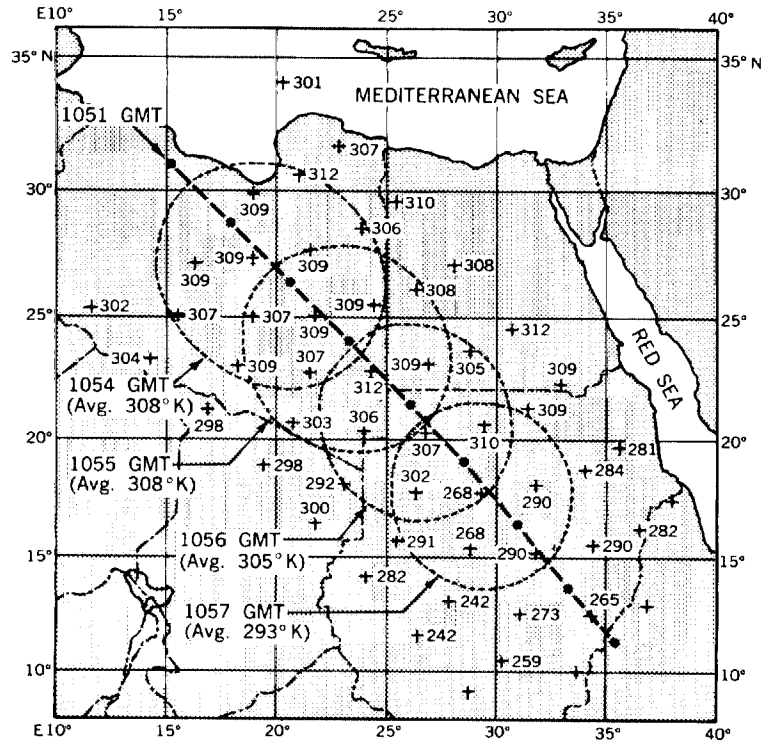

Figure 20—Effective blackbody temperatures (°K) measured by channel 2 (approximately 7.5 - 13.5μ) of the medium resolution radiometer between 1051 and 1057 GMT, Orbit 43, July 15, 1961. Averages of these data are given for the areas enclosed by dashed lines (also viewed by the low-resolution wide-field radiometer at the times shown). The heavy dashed line is the subsatellite path with points each minute.

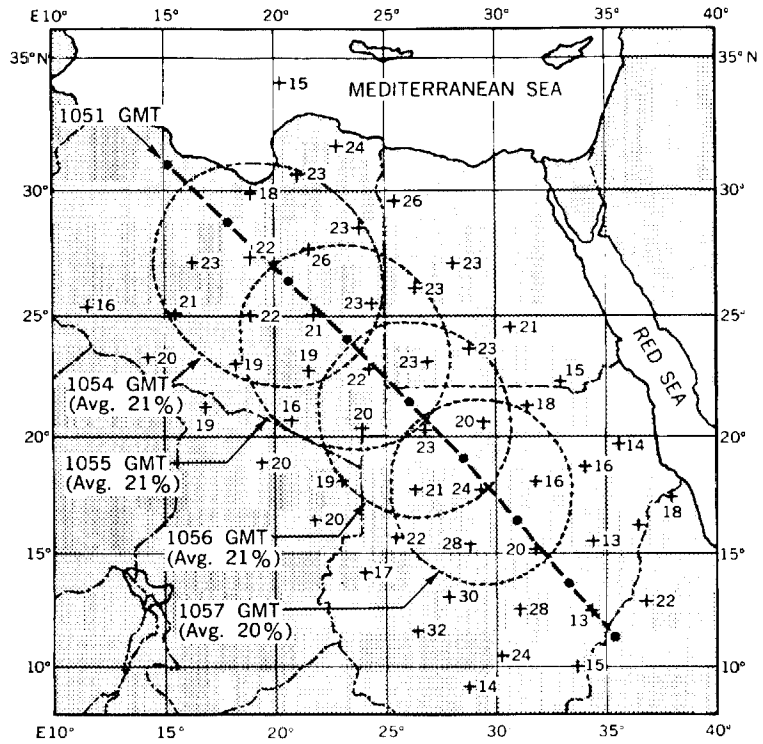

Figure 21—Albedo percentages measured by channel 3 (approximately 0.2 - 7.0μ) of the medium resolution radiometer between 1051 and 1057 GMT, Orbit 43, July 15, 1961. Averages of these data are given for the areas enclosed by dashed lines (also viewed by the low-resolution wide-field radiometer at the times shown). The heavy dashed line is the subsatellite path with points each minute.

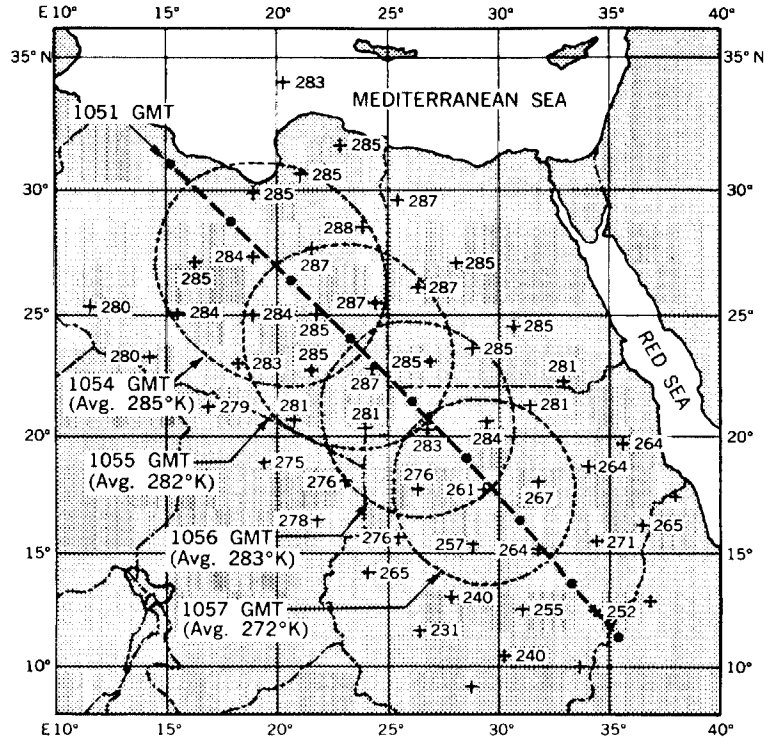

Figure 22—Effective blackbody temperatures (°K) measured by channel 4 (approximately 7.0 - 32.0μ) of the medium resolution radiometer between 1051 and 1057 GMT, Orbit 43, July 15, 1961. Averages of these data are given for the areas enclosed by dashed lines (also viewed by the low-resolution wide-field radiometer at the times shown). The heavy dashed line is the subsatellite path with points each minute.

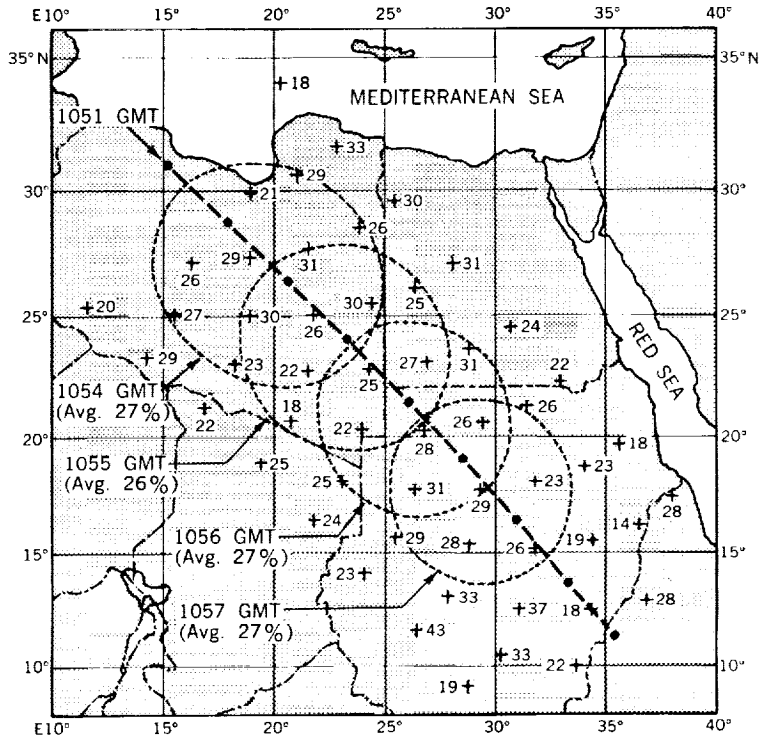

Figure 23—Albedo percentages measured by channel 5 (approximately 0.50 - 0.75μ) of the medium resolution radiometer between 1051 and 1057 GMT, Orbit 43, July 15, 1961. Averages of these data are given for the areas enclosed by dashed lines (also viewed by the low-resolution wide-field radiometer at the times shown). The heavy dashed line is the subsatellite path with points each minute.

appreciable water vapor. Over the same areas, the 5.9 to 6.7 and the 7.0 to 32.0 micron channels show apparent maximum blackbody temperatures of 260°K and 287°K, respectively (Figures 19 and 22). Again, this indicates a very high outward flux of energy due to the extremely low water vapor content over the desert. The wide-field instrument in this area also shows a maximum blackbody temperature of 305°K (Figure 24) at 1054 and 1055 GMT, which in this case is higher than the 7.0 to 32.0 micron channel temperatures.

At about 1057 GMT the picture changes abruptly. The apparent blackbody temperature from the wide-field radiometer plunges to approximately 260°K and remains there. This occurs when the field of view passes into the tropical regions of the Sudan near the 15th parallel. A similar drop also occurs in the three thermal channels. The average "window" channel temperature over the clear areas decreases to 290°K with minima as low as 280°K, while the 5.9 to 6.7 micron channel shows values as low as 230°K, (a drop of almost 30°K from the desert region), and the 7.0 to 32.0 micron channel averages read from about

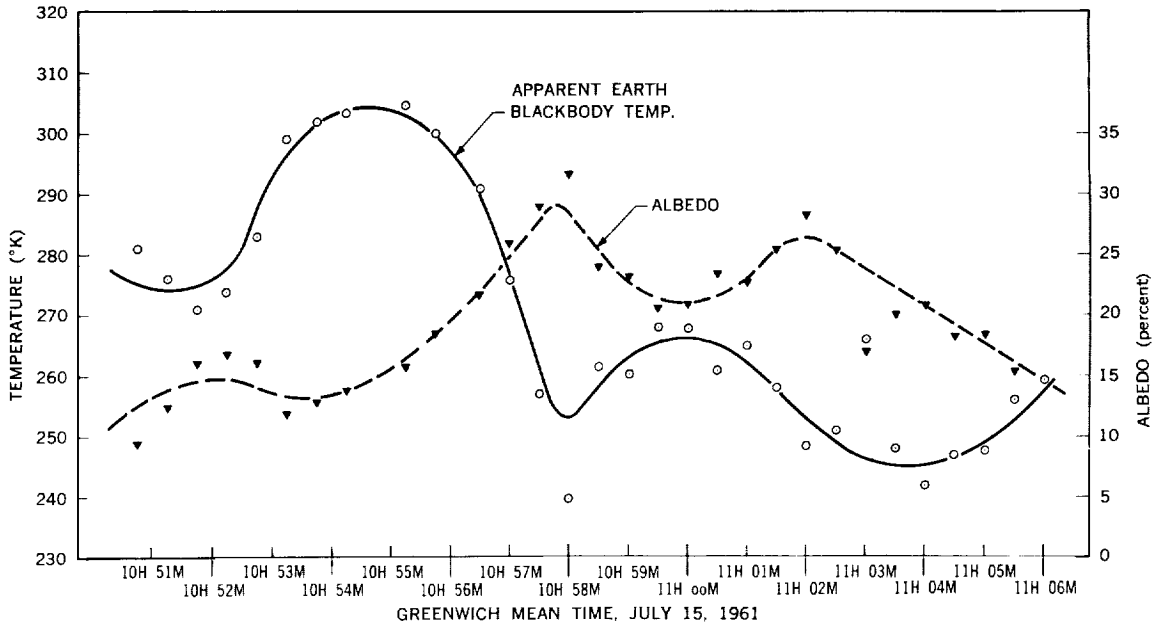

Figure 24—Apparent blackbody temperature and albedo versus time measured by the TIROS III wide-field radiometer during Orbit 43

270°K in the Blue Nile area to about 255°K in the Upper Nile area of the Sudan. This is again comparable to the wide-field temperatures in this area. It indicates a tremendous and rapid increase in atmospheric water vapor south of the 15th parallel and also demonstrates a remarkable decrease in outward energy flux when passing from the arid subtropical region into the tropical region.

CONCLUSION

The three simple cases presented here generally prove the consistency of the experiment and permit the following conclusions. The reflected solar radiation measurements for the 0.5 to 0.75 micron channel and the wide-field radiometer appear to be in good agreement. The measurements made in the 0.2 to 7.0 micron channel are consistently lower by an approximate factor of 0.75. It is conceivable that this is caused by a systematic error in the calibration source for the 0.2 to 7.0 micron channel.

Between 15 and 20 percent of incident solar radiation is reflected by moderately to heavily vegetated land under clear skies. There is good agreement in these values for all three cases, that is, the Northeast coast of South America, the Eastern United States, and the central Sudan. Values over the tropical Atlantic Ocean are very consistently near 7 percent under moderately calm conditions. (Wind speed readings from widely scattered stations indicate 10 to 15 knots.) Scattered clouds over the eastern United States and northeastern Africa indicate albedo values between 30 and 40 percent, while

values up to 55 percent were measured over a dense overcast above the east-central United States. Over the clear North African desert values between 25 and 30 percent are measured. Certain terrain features, such as mountain ranges in the desert, changes in climatic zones (going from arid to tropical), and shorelines of a continent can easily be distinguished by the reflected light channels of the medium resolution radiometer.

The observed blackbody temperatures measured in the various spectral regions representing outgoing radiation from the earth appear highly consistent. They indicate higher energy fluxes in the 7.5 to 13.5 micron "window" region than those given by the wide-field radiometer and the 7.0 to 32.0 micron channel and lower fluxes in the 5.9 to 6.7 water vapor absorption region. However, only over the African desert do the blackbody temperatures in the "window" region correspond to surface temperatures; in all other cases they are substantially lower (10° to 20°K). This implies that even in the "window" region as much as 25 percent of the outgoing energy may be absorbed by water vapor in the atmosphere.

Approximate total outward fluxes over a hemisphere can be calculated from the measured fluxes in the 7.0 to 32.0 micron channel by using the relation given by Wark and Yamamoto (Reference 8). They are: 192 w/m^2 over the East Central United States under heavily cloudy conditions, 250 w/m^2 over the tropical Atlantic Ocean in clear skies, 265 w/m^2 over the East Central United States in clear skies, and 340 w/m^2 over the desert in clear skies. These are the energy fluxes near local noon.

It is important to note that the observations over the tropical Atlantic which show the existence of a considerable energy surplus were made shortly after Hurricane Anna had developed in that same general area.

It may also be concluded from an analysis of these three cases, which constitute only a minute fraction of the total data available from TIROS III, that further investigation of the entire amount of data will produce a wealth of information, particularly in regard to energy fluxes as a function of time, geographic location, and meteorological conditions. Further theoretical studies are also needed to convert the limited information given by the sensors into total fluxes properly and more precisely.

The results stemming from these three cases strongly suggest that such radiation experiments could yield extremely interesting information when carried out on other planets.

REFERENCES

1. Hanel, R. A. and D. Q. Wark: "TIROS II Radiation Experiment and Its Physical Significance." Paper presented at the Optical Society of America Meeting, Pittsburgh, Pa., March 1961, and published as NASA Technical Note D-701.

2. Hanel, R. A., and Bandeen, W. R., "Some Results from the TIROS II Radiation Experiment." Paper presented at the International Association of Meteorology and Atmospheric Physics Symposia in Vienna, August 1961, and Tenth Pacific Science Congress, Honolulu, August 1961.

3. TIROS II Radiation Data Catalog. NASA, Goddard Space Flight Center, Greenbelt, Maryland, August 15, 1961.

4. Bandeen, W.R., Hanel, R.A., et al.: "Infrared and Reflected Solar Radiation Measurements from the TIROS II Meteorological Satellite." J. Geophys. Res., 65, 3169-3185, October 1961. Also published as NASA Technical Note D-1096, November 1961.

5. TIROS II Radiation Data User's Manual. NASA, Goddard Space Flight Center, Greenbelt, Maryland, August 15, 1961.

6. Hanel, R. A.: "Low Resolution Radiometer." ARS Journal, 31, 246-250, February 1961.

7. Davis, J., Hanel, R. A., et al.: "Telemetering IR Data from the TIROS II Meteorological Satellite." Paper presented at the IRE Professional Group on Space Electronics and Telemetry, Albuquerque, N. M., September 1961. Also published as NASA Technical Note D-1293, in press.

8. Wark, D. Q. and G. Yamamoto: "TIROS II Radiation Data and Their Meteorological Analysis." Paper presented at the International Association of Meteorology and Atmospheric Physics Symposia in Vienna, August 1961, and Tenth Pacific Science Congress, Honolulu, August 1961.